

# Effect of Sn crystallographic orientation on solder electromigration and Ni diffusion in Cu/Ni plating/Sn–0.7Cu joint at low current density

Takuya Kadoguchi<sup>1,2</sup> · Tsubasa Sakai<sup>3</sup> · Tsubasa Sei<sup>3</sup> · Naoya Take<sup>4</sup> · Kimihiro Yamanaka<sup>3</sup> · Shijo Nagao<sup>2</sup> · Katsuaki Suganuma<sup>2</sup>

Received: 11 December 2016 / Accepted: 5 May 2017 / Published online: 19 May 2017  
© Springer Science+Business Media New York 2017

**Abstract** Electromigration (EM) in solder joints has recently been recognized as a serious reliability issue in the field of car electronics. EM in power modules is also of concern for next-generation environmentally-friendly vehicles. The current density of 10 kA/cm<sup>2</sup> is well-known as the threshold for EM failure. Few researches have studied the EM behavior of solders at realistic current densities lower than 10 kA/cm<sup>2</sup>. In the present study, EM in a Cu/Ni plating/Sn–0.7Cu joint was investigated at low current densities of 2.5 and 5.0 kA/cm<sup>2</sup>. It was found that even at a low current density of 2.5 kA/cm<sup>2</sup>, severe EM damage can be induced depending on Sn crystallographic orientation. When the *c*-axis of Sn crystals was parallel to the direction of electron flow, the solder detached at the cathode of the joint operated at 2.5 kA/cm<sup>2</sup> for 2520 h. Conversely, when the *c*-axis of Sn crystals was perpendicular to the direction of electron flow, the solder did not detach in the joint until after a much longer time of 8200 h. Thus, it was clarified that the EM lifetime in a Cu/Ni plating/Sn–0.7Cu joint when the *c*-axis of Sn crystals was parallel to the direction of electron flow at a low current density of 2.5 kA/cm<sup>2</sup> was about one-third that of the perpendicular orientation.

## 1 Introduction

Electromigration (EM) in solder joints has been recognized as a reliability issue in electronics. In the field of semiconductors, EM has been studied extensively for decades to understand and control it in metallization. EM is the movement of metal atoms in the direction of electron flow, which is termed “electron wind”, and results from momentum transfer between conducting electrons and diffusing metal atoms. The mean time to failure shortens as the temperature or current density increases, which is expressed well by Black’s equation [1–4]. The current density of 10 kA/cm<sup>2</sup> is a well-known threshold for solder EM failure [4].

In the future, logic devices such as microprocessor units and graphic processing units will need to contain more than 10,000 input/output terminals to achieve the next level of performance. Therefore, solder joints of flip chips will soon need to be smaller than 50 μm in diameter, which will result in high electric current density in the solder joints [5].

In environmentally-friendly vehicles, including hybrid electric vehicles (HEVs), power modules with insulated gate bipolar transistors (IGBTs) and diodes operate alternating motors at currents above 200 A. Power modules are usually mounted in engine compartments, where the temperature is very high [6, 7]. Thus, power modules for HEVs are exposed to an environment where EM readily occurs. However, the current density of power semiconductors with solder in double-sided cooling power modules varies from 0.24 to 0.4 kA/cm<sup>2</sup> [8–10]. It is therefore believed that the influence of solder EM is minimal in this operating environment because the current density is less than 10 kA/cm<sup>2</sup>.

To make sufficient space for the driver and passengers, power modules for HEVs will be required to provide good fuel efficiency and high power density simultaneously [11, 12]. Power modules can be miniaturized by integrating

✉ Takuya Kadoguchi  
takuya\_kadoguchi@mail.toyota.co.jp

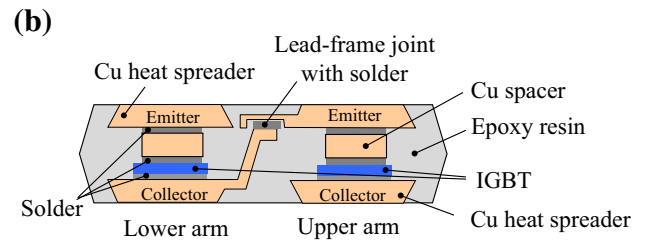
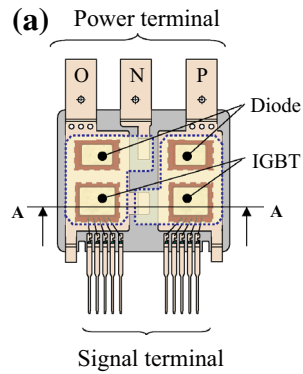
<sup>1</sup> Electronic Components Production Engineering Division, Toyota Motor Corporation, Hirose Plant, 543, Kirigahora, Nishihirose-cho, Toyota, Aichi 470-0309, Japan

<sup>2</sup> The Institute of Scientific and Industrial Research, Osaka University, 8-1, Mihogaoka, Ibaraki, Osaka 567-0047, Japan

<sup>3</sup> School of Engineering, Chukyo University, 101-2, Yagoto Honmachi, Showa, Nagoya, Aichi 466-8666, Japan

<sup>4</sup> Power Electronics Development Division, Toyota Motor Corporation, 1, Toyota-cho, Toyota, Aichi 471-8572, Japan

**Fig. 1** Schematic of the 2-in-1 power module for HEV. **a** Over view, **b** Cross-section of A-A line



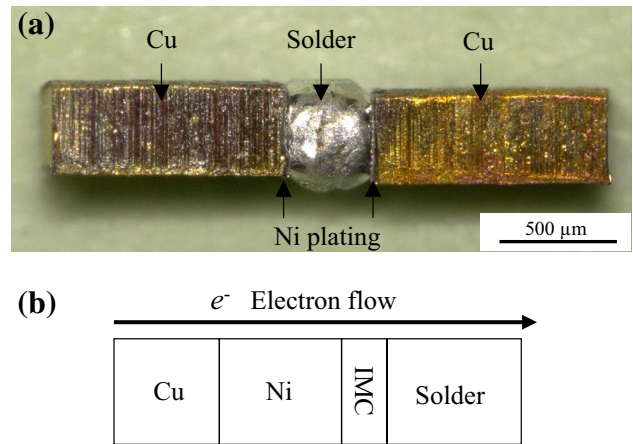
2-in-1 or 6-in-1 circuit compositions into one package. Figure 1a, b show schematic over view and cross-section of 2-in-1 power module for HEV where an emitter electrode in the upper arm IGBT is joined to a collector electrode in the lower arm IGBT with the solder [13, 14]. This lead-frame joint with solder is smaller than power semiconductors. The current density of the lead-frame joint becomes from 2.1 to 4.2 kA/cm<sup>2</sup> which displays approximately ten times higher than that of power semiconductors.

Extension of EM lifetime is a major research topic because it is well-understood that the complete suppression of EM is not practical. Previous researches have revealed that joints with under bump metallurgy, using materials such as Ni and Ni/Ti, enhance the EM reliability of Sn–Cu, Sn–Ag, and Sn–Pb solders at current densities higher than 10 kA/cm<sup>2</sup> [15–26]. However, few researches have studied the EM behavior of solders and Ni plating at realistic current densities lower than 10 kA/cm<sup>2</sup>. Therefore, here we investigated solder EM and Ni diffusion in Cu/Ni plating/Sn–0.7Cu joint at current densities lower than 10 kA/cm<sup>2</sup>.

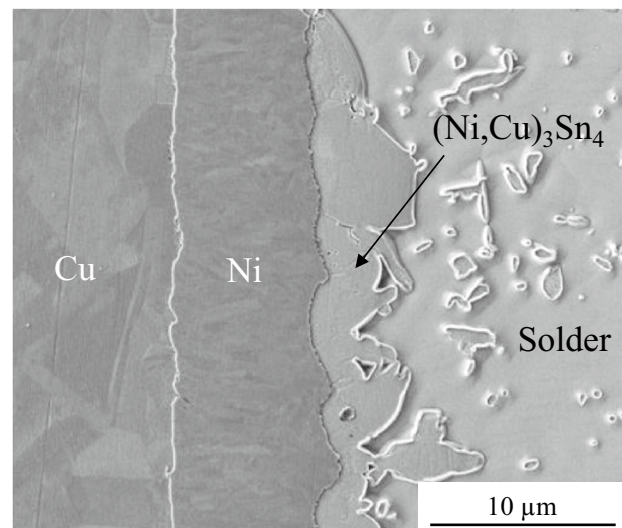
**2 Experimental procedure**

Figure 2a, b show a photograph of the sample and schematic cross-section of the cathode respectively. The electrodes were made of oxygen-free copper (C1020) and had a length of 1 mm and cross-section of 0.4×0.4 mm. The soldering pad for the Cu electrode was finished with electrolytic Ni/Au plating. The Ni plating was 7–13 μm thick. Two electrodes were joined with a solder ball in a diameter of 0.5 mm. The solder was M725 (Sn–0.7Cu–Ni–P, wt%; Senjyu Metal Industry Co., Ltd.).

Figure 3 shows a scanning electron microscope (SEM) image of the cross-section of a joint interface. The intermetallic compound (IMC) at the interface was about 4.5 μm thick. Ni plating was ~9.0 μm thick after reflow. Energy-dispersive X-ray spectroscopy (EDX) showed that the IMC consisted of 34.4 at.% Ni–8.9 at.% Cu–56.7 at.% Sn. Thus,



**Fig. 2** **a** Photograph of the sample joint, **b** Schematic of the cathode side. The arrow shows the electron flow direction



**Fig. 3** Cross-sectional SEM image of the solder joint interface after reflow

the estimated IMC composition was  $(\text{Ni,Cu})_3\text{Sn}_4$ , confirming the sample composition in Fig. 2b.

We applied currents of 4.0 and 8.0 A to solder joints to generate current densities of 2.5 and 5.0  $\text{kA/cm}^2$  respectively. Each test sample was placed on a hot plate that maintained the joint temperature at 150 °C when applying direct current through the joint. The temperature profile of the test sample was measured by a thermocouple. The thermocouple was placed on one Cu electrode of the test sample. The change in resistance caused by EM was measured by monitoring the voltage in the junction line between Cu/solder/Cu joints. We defined the failure criterion as a 20% increase in resistance from the initial value.

To study the EM behavior of solder joints, we analyzed them after applying a current density of 2.5  $\text{kA/cm}^2$  at 150 °C for 250, 750, and 1000 h. Cross-sections of test samples were polished and studied using SEM, EDX, and electron backscattered diffraction (EBSD) to measure the Sn crystal orientation. Previous researches report the control of the crystallographic orientation of Sn grains is important after soldering [27, 28]. It is assumed that EM will not affect the crystallographic orientation of Sn grains. Therefore, the crystallographic orientation of Sn grains was indexed after EM stress test. Figure 4 shows the relationship between the cross-section of the solder and direction of observation. The direction of observation is the normal direction (ND) and electron flow is the transverse direction (TD).

We checked for dissipation of the Ni plating in the test sample with SEM. Ni plating dissipation  $\Delta i$  is defined as:

$$\Delta i = d_0 - d_i,$$

where  $d_0$  is the initial thickness of the Ni plating and  $d_i$  is the average thickness of the Ni plating after EM stress test. The thickness of the Ni plating was measured at ten locations.

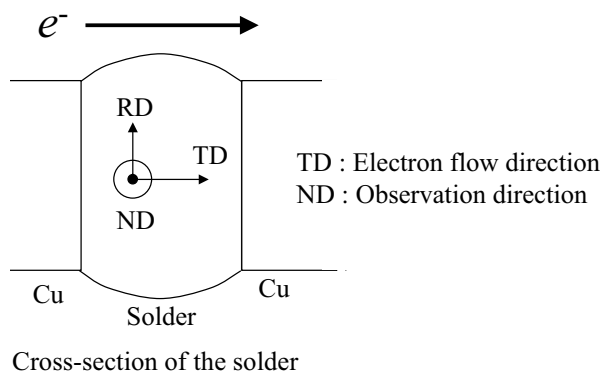


**Fig. 4** Observation and electron flow directions of Sn crystallographic orientation

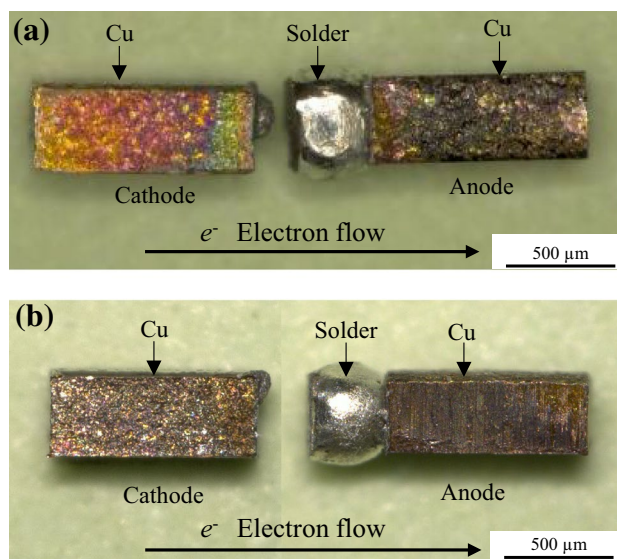
### 3 Results and discussion

#### 3.1 Electromigration failure mode at low current densities

Applying current densities of 5.0 and 2.5  $\text{kA/cm}^2$  to samples heated at 150 °C resulted in failure times of 950 and 2520 h respectively. Figure 5a, b show photographs of failed samples after EM stress test. The solders detached from the Cu cathode respectively. This trend agrees with a previous research that reported the EM breakdown mode in a Cu/Ni–P/Sn–0.7Cu joint at a current density of 5.0  $\text{kA/cm}^2$  [29].

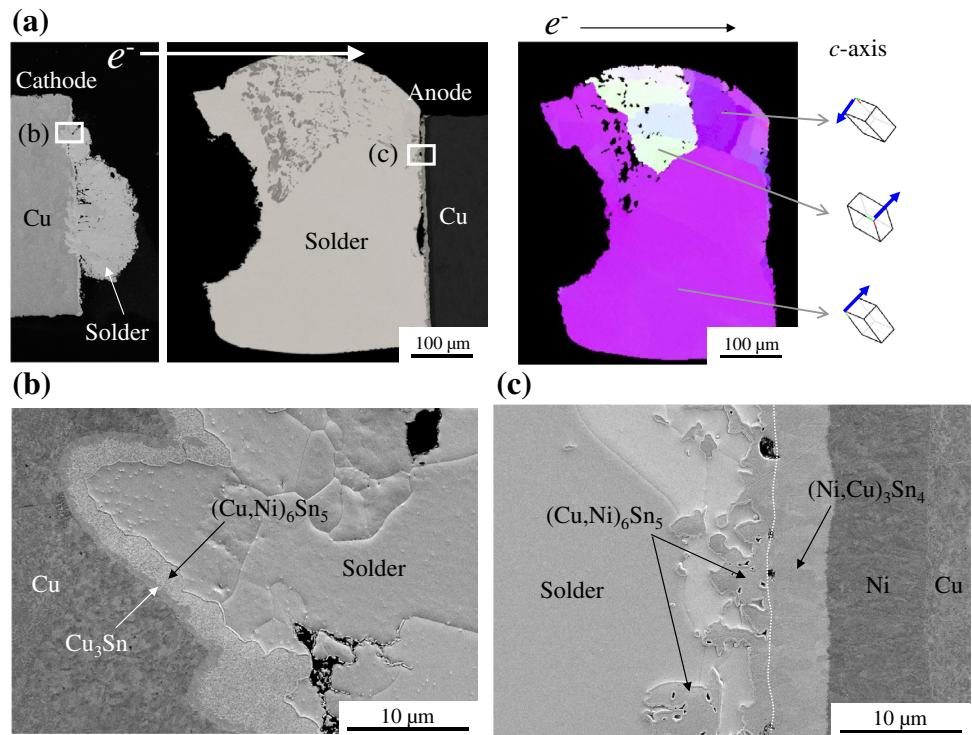
Figure 6a shows cross-sectional SEM (left) and EBSD (right) images of the sample stressed at 5.0  $\text{kA/cm}^2$  and 150 °C for 950 h. In the EBSD image, the orientation of large grains is shown by arrows in the unit cell indicating the  $c$ -axes of Sn crystals. The  $c$ -axis of Sn crystals for the TD was 44.1°. The  $c$ -axes of Sn crystals was nearly parallel to the electron flow. Figure 6b shows enlarged SEM image of the cathode. Ni plating that remained after reflow disappeared. The Cu electrode reacted with Sn to form  $\text{Cu}_3\text{Sn}$  and  $(\text{Cu,Ni})_6\text{Sn}_5$  IMCs. Figure 6c shows an enlarged SEM image of the anode. The layer of  $(\text{Ni,Cu})_3\text{Sn}_4$  IMC slightly grew thicker during the EM stress test and was about 4.9  $\mu\text{m}$ . In addition, a  $(\text{Cu,Ni})_6\text{Sn}_5$  IMC layer continuously formed on  $(\text{Ni,Cu})_3\text{Sn}_4$  until it was about 4.2  $\mu\text{m}$  thick. Cu and Sn atoms in the  $(\text{Cu,Ni})_6\text{Sn}_5$  IMC at the cathode or in the solder can be transferred by the electron flow.

Figure 7a shows cross-sectional SEM (left) and EBSD (right) images of the sample stressed at 2.5  $\text{kA/cm}^2$  and

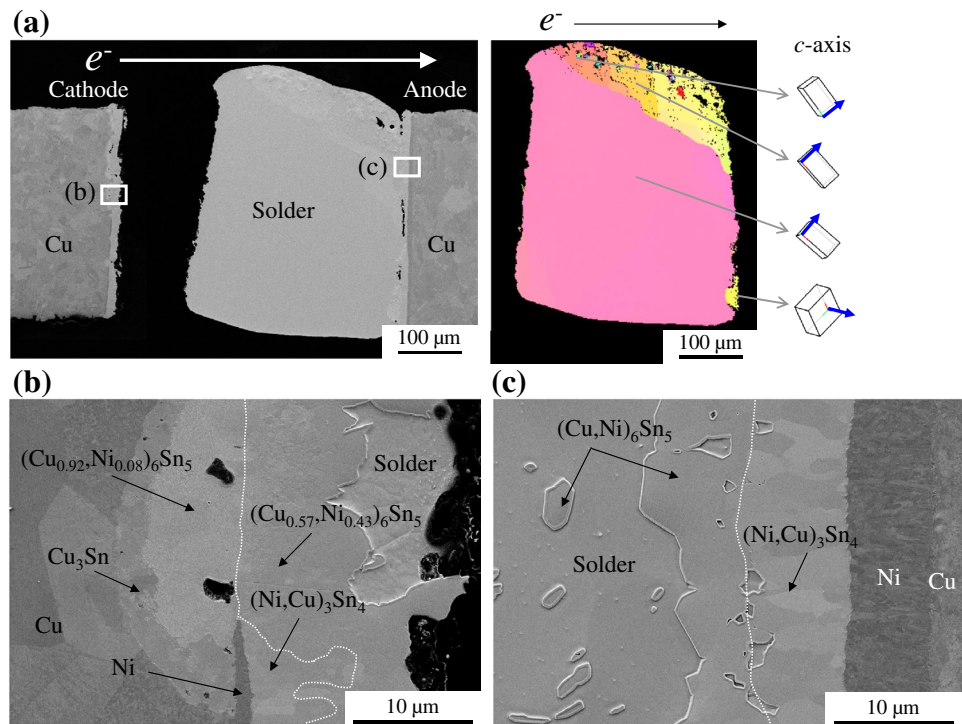


**Fig. 5** Photographs of failed samples after operation at **a** 5.0  $\text{kA/cm}^2$  and 150 °C for 950 h and **b** 2.5  $\text{kA/cm}^2$  and 150 °C for 2520 h

**Fig. 6** **a** Cross-sectional SEM (left) and EBSD (right) images of a solder joint after 950 h at 5.0 kA/cm<sup>2</sup> and 150 °C. Enlarged SEM images of the **b** cathode side and **c** anode side. In the EBSD image, the orientation of large grains is marked by arrows in the unit cells indicating the *c*-axes of the Sn crystals



**Fig. 7** **a** Cross-sectional SEM (left) and EBSD (right) images of a solder joint after 2520 h at 2.5 kA/cm<sup>2</sup> and 150 °C. Enlarged SEM images of the **b** cathode side and **c** anode side



150 °C for 2520 h. The *c*-axes of Sn crystals for the TD were from 37.1° to 44.5°. The *c*-axes of Sn crystals were nearly parallel to the electron flow. Figure 7b shows an enlarged SEM image of the cathode. The breakdown

interface was in the solder and between the solder and (Cu<sub>0.57</sub>Ni<sub>0.43</sub>)<sub>6</sub>Sn<sub>5</sub> IMC. Sn atoms in the solder were transferred by the electron flow, resulting in the formation of voids at the cathode interface. Ni plating that remained

after reflow disappeared or became thin (about  $1.0\ \mu\text{m}$  thick). The Cu electrode where Ni plating disappeared reacted with Sn to form  $\text{Cu}_3\text{Sn}$  and  $(\text{Cu}_{0.92}\text{Ni}_{0.08})_6\text{Sn}_5$  IMCs. The  $(\text{Ni,Cu})_3\text{Sn}_4$  IMC remained on a thin Ni plating layer after EM stress test, and was about  $7.5\ \mu\text{m}$  thick. The layer of  $(\text{Ni,Cu})_3\text{Sn}_4$  IMC grew thicker after EM stress test. Figure 7c shows an enlarged SEM image of the anode. The layer of  $(\text{Ni,Cu})_3\text{Sn}_4$  IMC grew thicker during EM stress test, and was about  $6.2\ \mu\text{m}$  thick. In addition, a  $(\text{Cu,Ni})_6\text{Sn}_5$  IMC layer continuously formed on  $(\text{Ni,Cu})_3\text{Sn}_4$  until it was about  $5.7\ \mu\text{m}$  thick. Cu and Sn atoms in the  $(\text{Cu,Ni})_3\text{Sn}_4$  IMC at the cathode or in the solder can be transferred by the electron flow. The Ni plating was about  $6.4\ \mu\text{m}$  thick, and became thinner compared with that after reflow. These results agreed with those at  $5.0\ \text{kA/cm}^2$  and  $150\ ^\circ\text{C}$ , as indicated in Fig. 6c.

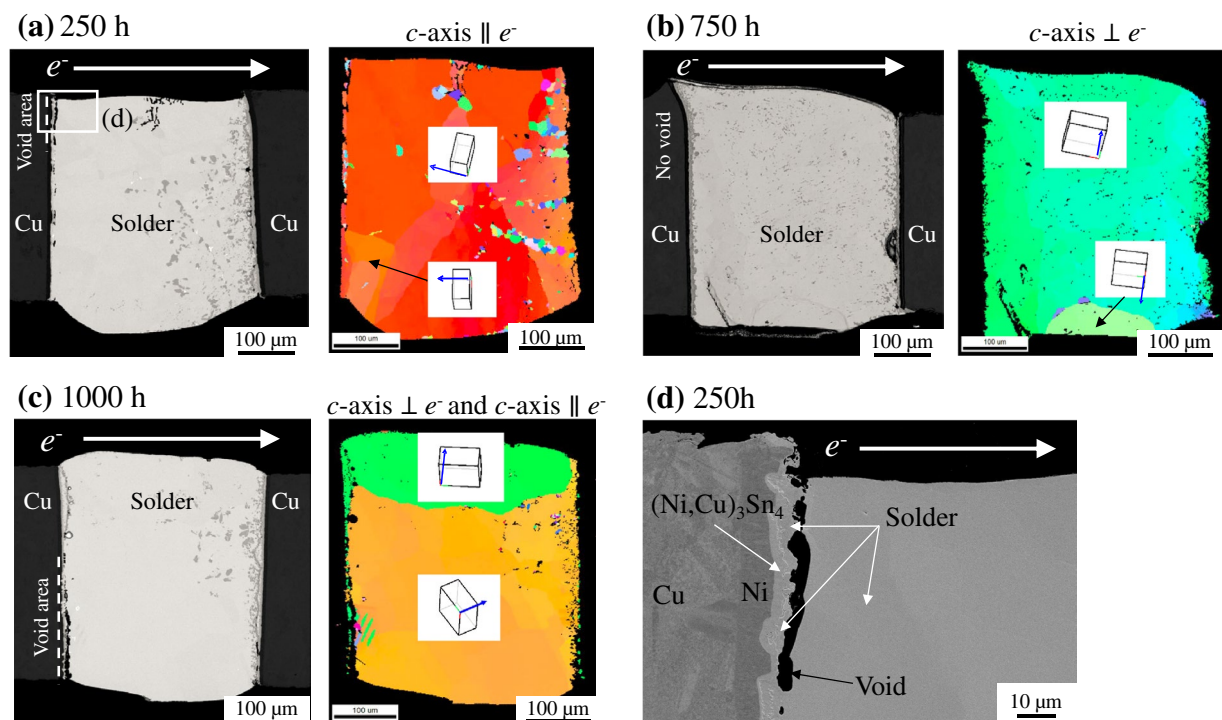
Ni atoms in the Ni plating at the cathode were transferred by EM and thermal diffusion. As a result, more Ni plating disappeared at the cathode than at the anode. Thus, EM accelerated the Ni diffusion in the Ni plating at the cathode toward the solder.

### 3.2 Effect of Sn crystallographic orientation on EM behavior

Figure 8 shows cross-sectional SEM (left) and EBSD (right) images of the solder joint after EM testing at

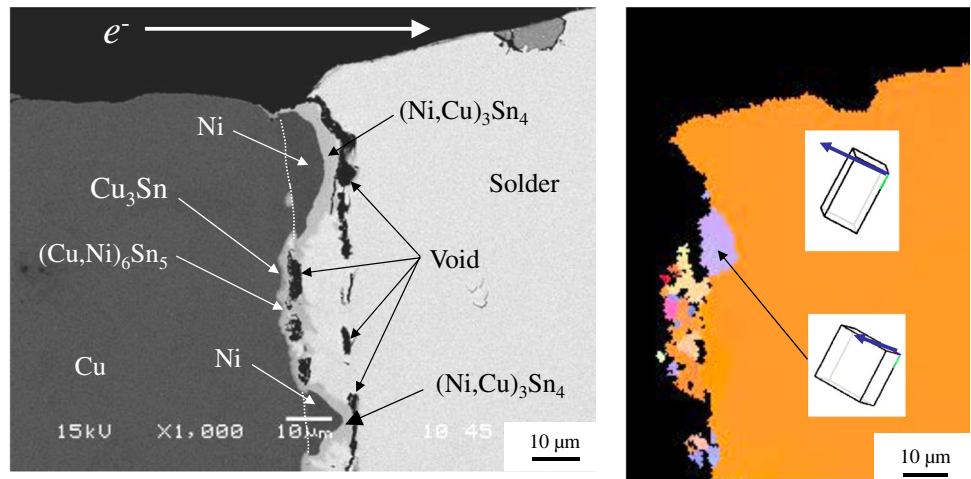
$2.5\ \text{kA/cm}^2$  and  $150\ ^\circ\text{C}$ . No samples exceeded the failure criterion of a 20% increase in resistance from the initial value. The void area is indicated by a dashed line in SEM images. A void was observed at the cathode after 250 and 1000 h, but no void was detected after 750 h. The  $c$ -axes of Sn crystals in the sample after 250 h were parallel to the direction of electron flow ( $c\text{-axis} \parallel e^-$ ). Conversely, the  $c$ -axes of Sn crystals after 750 h were perpendicular to the direction of electron flow ( $c\text{-axis} \perp e^-$ ). Figure 8c reveals that the  $c$ -axes of Sn crystals after 1000 h had regions both perpendicular ( $c\text{-axis} \perp e^-$ ) and parallel ( $c\text{-axis} \parallel e^-$ ) to the direction of electron flow. The parallel region had a continuous void between the solder and Cu electrode, while the perpendicular region had no void. The void formed in the solder and between the  $(\text{Ni,Cu})_3\text{Sn}_4$  IMC and solder at the cathode is shown in Fig. 8d. The void formation in the solder resulted from EM of Sn atoms toward the solder at the anode and thermal diffusion of Sn atoms toward the Ni plating at the cathode.

Figure 9 shows cross-sectional SEM (left) and EBSD (right) images of the solder joint at the cathode after 250 h at  $5.0\ \text{kA/cm}^2$  and  $150\ ^\circ\text{C}$ . This sample did not exceed the failure criterion of a 20% increase in resistance from the initial value. The  $c$ -axes of Sn crystals were nearly parallel to the direction of electron flow. The void formed in the solder and between  $(\text{Ni,Cu})_3\text{Sn}_4$  IMC and the solder. This result agreed with that at  $2.5\ \text{kA/cm}^2$



**Fig. 8** Cross-sectional SEM (left) and EBSD (right) images of a solder joint operated at  $2.5\ \text{kA/cm}^2$  and  $150\ ^\circ\text{C}$  for **a** 250 h, **b** 750 h, and **c** 1000 h. **d** Enlarged SEM image of the cathode side for **a** 250 h

**Fig. 9** Cross-sectional SEM (left) and EBSD (right) images of a solder joint after 250 h at 5.0 kA/cm<sup>2</sup> and 150 °C

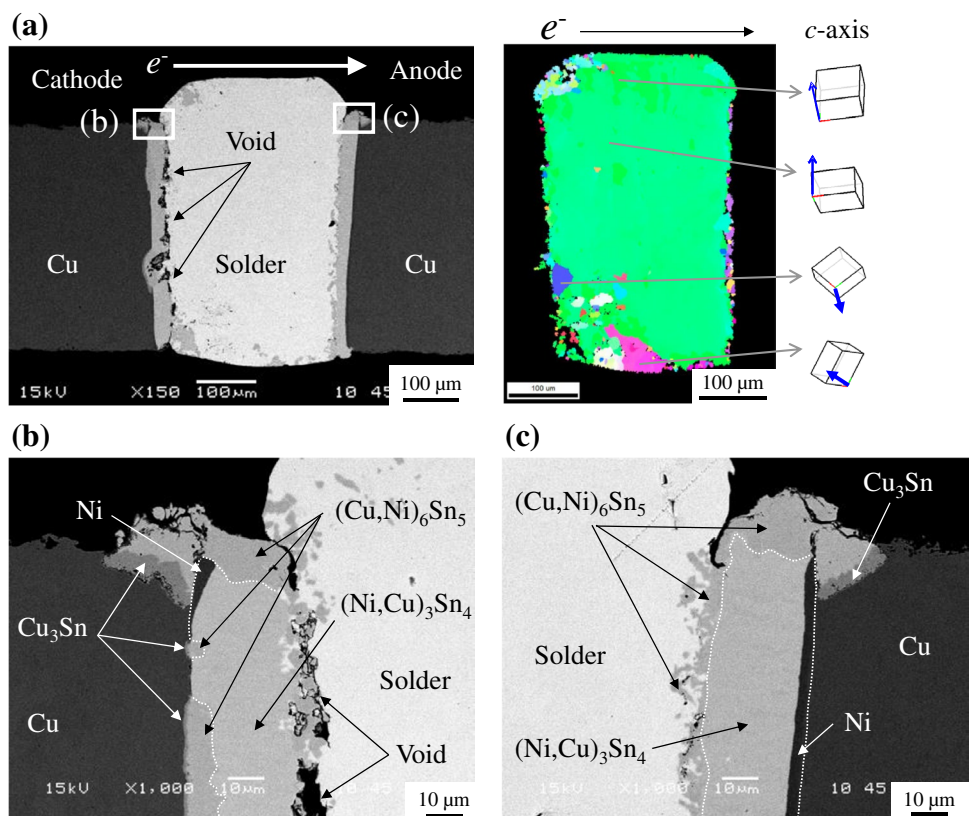


cm<sup>2</sup>, as indicated in Fig. 8d. The Cu electrode where Ni plating disappeared reacted with Sn to form Cu<sub>3</sub>Sn and (Cu,Ni)<sub>6</sub>Sn<sub>5</sub> IMCs. The electron flow at higher current density of 5.0 kA/cm<sup>2</sup> accelerated the Ni diffusion in the Ni plating at the cathode toward the solder. Further the void formed between (Cu,Ni)<sub>6</sub>Sn<sub>5</sub> IMC and the solder. The void formation resulted from EM of Sn atoms toward the anode and thermal diffusion of Sn atoms toward the Cu electrode at the cathode after Ni plating disappeared. Thus, voids appeared in the regions parallel to the

direction of electron flow even at a lower current density than 10 kA/cm<sup>2</sup>.

We also applied a current density of 2.5 kA/cm<sup>2</sup> to another sample at 150 °C for 8200 h. This sample did not exceed the failure criterion of a 20% increase in resistance from the initial value. Cross-sectional SEM (left) and EBSD (right) images of a solder joint after operating for 8200 h at 2.5 kA/cm<sup>2</sup> and 150 °C are shown in Fig. 10a. The solder did not detach from the Cu electrode, although voids formed at the cathode side. The

**Fig. 10 a** Cross-sectional SEM (left) and EBSD (right) images of a solder joint after 8200 h operating at 2.5 kA/cm<sup>2</sup> and 150 °C. Enlarged SEM images of the **b** cathode side and **c** anode side



*c*-axes of Sn crystals for the TD were from 80.8° to 87.1° and were nearly perpendicular to the electron flow. Figure 10b shows an enlarged SEM image of the cathode. A void formed between the solder and (Ni,Cu)<sub>3</sub>Sn<sub>4</sub> IMC. Ni plating at the cathode reacted the solder, resulting in the growth of a (Ni,Cu)<sub>3</sub>Sn<sub>4</sub> IMC. The Cu electrode formed Cu<sub>3</sub>Sn and (Cu,Ni)<sub>6</sub>Sn<sub>5</sub> IMCs because of the disappearance of the Ni plating. An enlarged SEM of the anode is shown in Fig. 10c. The layer of (Ni,Cu)<sub>3</sub>Sn<sub>4</sub> IMC was about 25 μm thick, which was thicker compared with that after operating for 2520 h, as indicated in Fig. 7c. Ni plating at the anode remained about 2.8 μm thick, and became thinner compared with that after reflow.

Thus, EM damage after 8200 h was smaller compared with that after 2520 h, as indicated in Fig. 7a. The EM damage depended on Sn crystallographic orientation. The crystal anisotropy in Sn, which is a major component in lead-free solder, is focused on here. Sn has a body-centered tetragonal crystal structure with lattice constants of  $a=b=0.583$  nm and  $c=0.318$  nm, and displays highly anisotropic diffusion with respect to the axis direction [30, 31]. For example, the diffusivity of Cu atoms along the *c*-axis of Sn crystals is approximately forty times faster than that along the *a*-axis at 160 °C [32]. Thus, very fast development of EM behavior has been observed along the *c*-axis compared with that along the *a* and *b*-axes.

In the present study, the EM lifetime decreased by about one-third even at a low current density of 2.5 kA/cm<sup>2</sup> when the *c*-axis of Sn crystals was parallel to the direction of electron flow. Thus, it was clarified that Sn orientation

direction affected EM lifetime even at a current density lower than 10 kA/cm<sup>2</sup>.

### 3.3 Dependence of Ni diffusion behavior in the Ni plating on Sn crystallographic orientation

We investigated the Ni diffusion in the Ni plating toward the solder at a current density of 2.5 kA/cm<sup>2</sup>. Figure 11a shows a cross-sectional SEM image of the solder joint after operating for 1000 h at 2.5 kA/cm<sup>2</sup> and 150 °C. Meanwhile, Fig. 11b shows enlarged SEM (left) and EBSD (right) images that reveal the *c*-axis of Sn crystals on the Ni plating was perpendicular to the electron flow. The Ni plating was about 5.9 μm thick, which was thinner compared with that after reflow. However, the Ni plating became thin (about 3.6 μm thick) and discontinuous, as shown in Fig. 11c. The *c*-axis of Sn crystals on the Ni plating was parallel to the electron flow. Thus, the *c*-axis of Sn crystals appeared to affect not only the rate of Sn diffusion toward the solder but also that of Ni diffusion.

Figure 12 shows the dissolution thickness of the Ni plating and the thickness of (Ni,Cu)<sub>3</sub>Sn<sub>4</sub> IMC over different Sn crystal orientations after operating for 1000 h at 2.5 kA/cm<sup>2</sup> and 150 °C. The dissolution thickness of Ni plating in the perpendicular region at the cathode was 1.1 μm, and was nearly as the same as that of the anneal-only sample. However, the dissolution thickness in the parallel region at the cathode was 3.4 μm, which was about three times thicker than that in the perpendicular region. The dissolution thickness in the parallel region at the anode was 0.6 μm, which

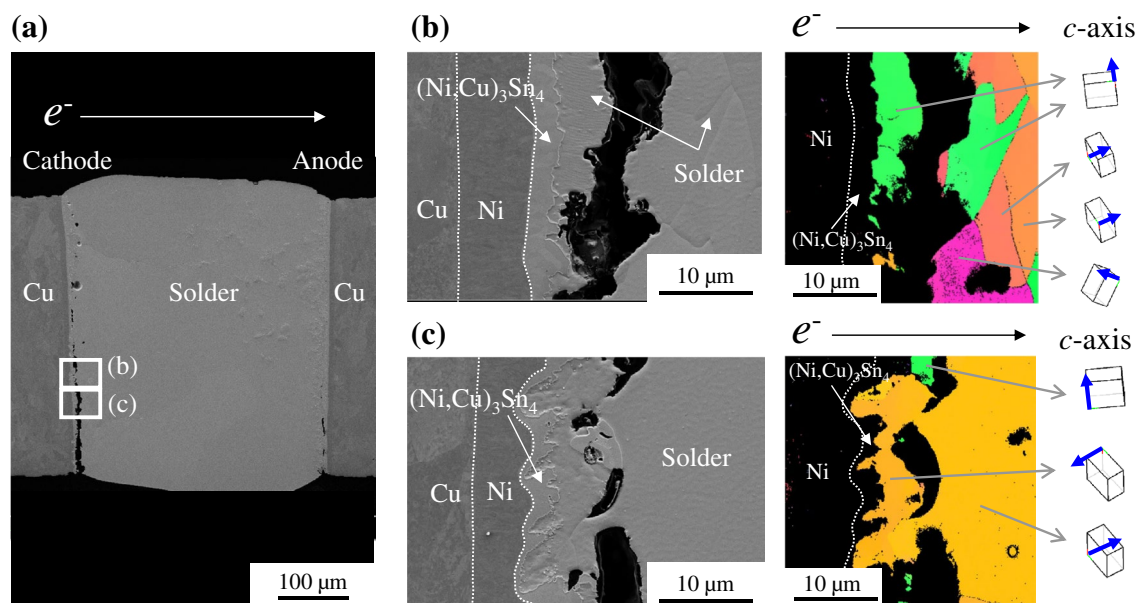


**Fig. 11** **a** Cross-sectional SEM image of a solder joint after 1000 h operating at 2.5 kA/cm<sup>2</sup> and 150 °C. **b, c** Enlarged SEM (*left*) and EBSD (*right*) images of the solder

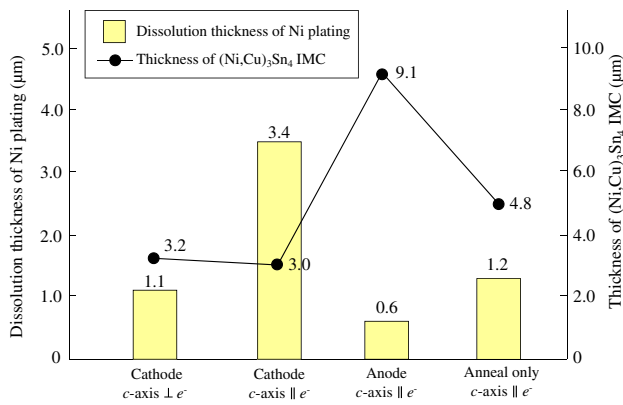


**Fig. 12** Dissolution thickness of the Ni plating and thickness of (Ni,Cu)<sub>3</sub>Sn<sub>4</sub> IMC over different Sn orientations after 1000 h operating at 2.5 kA/cm<sup>2</sup> and 150 °C

was as half that of the anneal-only sample. It has been reported that the rate of Ni diffusion along Sn atoms in the parallel region is seventy thousand times faster than that in the perpendicular region [33], which is corroborated by the trend in the present study. Thus, at the cathode, EM accelerated the Ni diffusion in the parallel region even at a current density lower than 10 kA/cm<sup>2</sup>. At the anode, EM suppressed Ni diffusion compared with that at the cathode and for the anneal-only sample.

The thickness of (Ni,Cu)<sub>3</sub>Sn<sub>4</sub> IMC in the perpendicular region at the cathode was about 3.2 µm and was nearly as the same as that in the parallel region at the cathode. The thickness of (Ni,Cu)<sub>3</sub>Sn<sub>4</sub> IMC in the parallel region at the anode was about 9.1 µm and was thicker than that at the cathode and of the anneal-only sample.

Although EM suppressed Ni dissolution at the anode, the (Ni,Cu)<sub>3</sub>Sn<sub>4</sub> IMC at the anode was thicker because of the migration of Ni, Cu and Sn atoms from the cathode. Meanwhile, although EM accelerated Ni dissolution in the parallel region at the cathode, the thickness of (Ni,Cu)<sub>3</sub>Sn<sub>4</sub> IMC was as the same as that in the perpendicular region. It was speculated that Ni of the Ni plating in the parallel region at the cathode migrated toward the anode instead of the growth of IMC at the cathode.

Thus, at the cathode, EM suppressed the growth the (Ni,Cu)<sub>3</sub>Sn<sub>4</sub> IMC regardless of Sn crystallographic orientation. At the anode, EM accelerated the growth of IMC compared with that at the cathode and for the anneal-only sample even at a current density lower than 10 kA/cm<sup>2</sup>.

### 3.4 Breakdown mechanism of the cathode during EM stress testing

Figure 13 shows a schematic of the damage process with respect to the axis direction of Sn crystals at the cathode

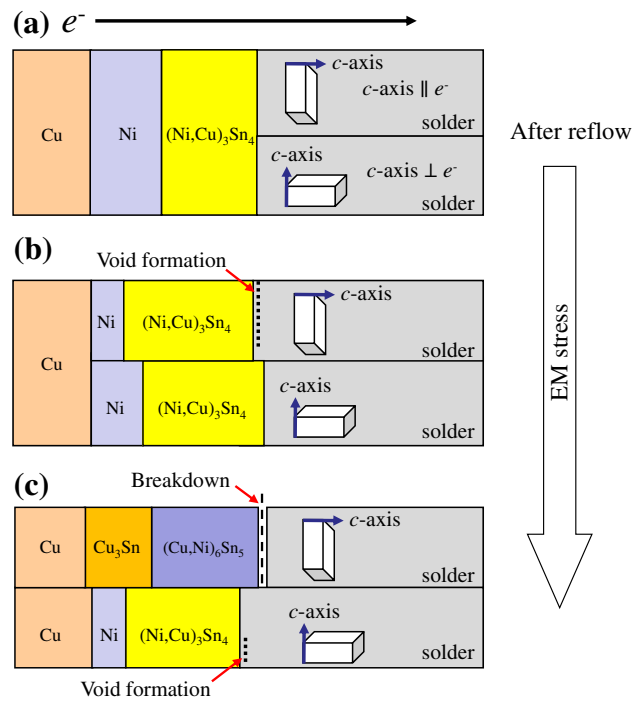


**Fig. 13** Schematic of the damage process with respect to the axis direction of Sn crystals at the cathode after EM stress. **a** after reflow, **b, c** void formation and breakdown mode

during EM stress test. A (Ni,Cu)<sub>3</sub>Sn<sub>4</sub> IMC formed at the Ni plating interface after reflow. When the *c*-axis of Sn crystals was parallel to the electron flow, EM accelerated the Ni diffusion in the Ni plating and the transfer of Sn atoms from the solder, resulting in void formation. Furthermore, EM stress caused the Ni plating to disappear and Sn reacted with the Cu electrode to form Cu<sub>3</sub>Sn and (Cu,Ni)<sub>6</sub>Sn<sub>5</sub>. Finally, breakdown occurred between the solder and (Cu,Ni)<sub>6</sub>Sn<sub>5</sub> IMC. When the *c*-axis of Sn crystals was perpendicular to the electron flow, the rate of Ni diffusion under EM stress was as the same as that for the anneal-only sample. The rate of void formation at the solder interface was slow and the effect of EM was very small.

## 4 Conclusions

In the present study, to investigate the EM behavior of a solder, current densities of 5.0 and 2.5 kA/cm<sup>2</sup> were applied to a Cu/Ni plating/Sn–0.7Cu joint at 150 °C. The failure times for joints exposed to current densities of 5.0 and 2.5 kA/cm<sup>2</sup> were 950 and 2520 h respectively. The breakdown interface was in the solder or between the solder and (Cu,Ni)<sub>6</sub>Sn<sub>5</sub> IMC at the cathode. Ni plating at the cathode disappeared or became thinner compared with that after



reflow. The Cu electrode reacted with Sn and formed  $\text{Cu}_3\text{Sn}$  and  $(\text{Cu},\text{Ni})_6\text{Sn}_5$  IMCs after the Ni plating disappeared. Ni plating at the anode became slightly thinner compared with that after reflow. The region where the  $c$ -axis of Sn crystals was parallel to the direction of electron flow had a continuous void between the solder and  $(\text{Cu},\text{Ni})_6\text{Sn}_5$  IMC. In contrast, the region where the  $c$ -axis of Sn crystals was perpendicular to the direction of electron flow had no void after EM stress testing for 1000 h. Thus, the sample containing the latter region displayed a long lifetime of 8200 h in EM tests. EM accelerated the rate of Ni diffusion in the Ni plating at the cathode region where the  $c$ -axis of Sn crystals was parallel to the direction of electron flow. At the anode, EM suppressed Ni diffusion compared with that observed at the cathode and for the anneal-only sample at 150 °C. However, at the cathode, EM suppressed the growth the  $(\text{Ni},\text{Cu})_3\text{Sn}_4$  IMC regardless of Sn crystallographic orientation. At the anode, EM accelerated the growth of IMC compared with that at the cathode and for the anneal-only sample. Thus, the relationship between the  $c$ -axis of Sn crystals and the direction of electron flow affected the rate of Ni diffusion in the Ni plating toward the solder at the cathode. Overall, we clarified that the EM lifetime in a Cu/Ni plating/Sn–0.7Cu joint became shorter at a current density lower than 10 kA/cm<sup>2</sup> when the  $c$ -axis of Sn crystals was parallel to the direction of electron flow.

**Acknowledgements** The authors would like to acknowledge that part of this research was performed with financial support from the Chukyo University Research Fund.

## References

- J.R Black, Electromigration- a brief survey and some recent results. *IEEE Trans. Electron. Dev.* **16**(4), 338 (1969)
- J.R Black, Physics of electromigration. In: Proceedings of reliability physics, p. 142 (1974)
- J.R Black, Electromigration of Al-Si Alloy films. In: Proceedings of reliability physics, p. 300 (1978)
- K.N. Tu, Recent advances on electromigration in very-large-scale-integration of interconnects. *J. Appl. Phys.* **94**(9), 5451 (2003)
- ITRS2011 (International Technology Roadmap for semiconductors), <http://www.itrs.net/Links/2011ITRS/Home2011.htm>
- T. Matsubara, H. Yaguchi, T. Takaoka, et al. Development of new hybrid system for compact class vehicle. In: Proceedings of JSAE2009, Japan, p. 21 (2009)
- N. Nozawa, T. Maekawa, E. Yagi, et al. Development of Power Control Unit for compact class vehicle. In: Proceedings of 22nd ISPSD 2010, Japan, p. 43 (2010)
- S. Miura, Y. Ookura, Y. Okabe, et al., Development of power devices for power cards. *Denso Tech. Rev.* **16**, 38 (2011)
- N. Hirano, K. Mamitsu, T. Okumura, Structural development of double-sided cooling power modules. *Denso Tech. Rev.* **16**, 30 (2011)
- Y. Sakamoto, Assembly technologies of double-sided cooling power modules. *Denso Tech. Rev.* **16**, 46 (2011)
- K. Hamada, Present status a future prospects for electronics in EVs/HEVs and expectations for wide bandgap semiconductor devices. *Mater. Sci. Forum.* **600–603**, 889 (2009)
- S. Hirose, Power electronics technology for the next generation environmentally-friendly vehicles. In: Proceedings of the 24th Microelectronics Symposium, JIEP, Japan, p. 37 (2014) (Japanese)
- O. Kitazawa, T. Kikuchi, M. Nakashima et al., Development of power control unit for compact-class vehicle. *SAE Int. J. Alt. Power* **5**(2), 278 (2016)
- S. Hushiki, M. Taniguchi, K. Takizawa, et al., Hybrid technologies for the new prius. *TOYOTA Tech. Rev.* **62**, 61 (2016)
- L.N. Ramanathan, T.-Y.T. Lee, J.-W. Jang, et al., Current carrying capability of Sn0.7Cu solder bumps in flip chip modules for high power applications In: Proceedings of 57th ECTC 2007, Reno, p. 1456 (2007)
- K. Yamanaka, Y. Tsukada, K. Sugauma, Soder electromigration in Cu/In/Cu flip chip joint system. *J. Alloys Compd.* **437**, 186 (2007)
- K. Yamanaka, Y. Tsukada, K. Sugauma, Studies on solder bump electromigration in Cu/Sn-3Ag-0.5Cu/Cu system. *Microelectron. Reliab.* **47**, 1280 (2007)
- M. Lu, P. Lauro, D.-Y. Shih, R. Polastre, et al., Comparison of electromigration performance for Pb-free solders and surface finishes with Ni UBM. In: Proceedings of 58th ECTC 2008, Orlando, p. 360 (2008)
- S.-H. Chael, J. Im, T. Uehling, et al., Effects of UBM thickness, contact trace structure and solder joint scaling on electromigration reliability of Pb-free solder joints. In: Proceedings of 58th ECTC 2008, Orlando, p. 354 (2008)
- Y.-S. Lai, Y.-T. Chiu, C.-W. Lee, et al., Electromigration reliability and morphologies of Cu pillar flip-chip solder joints. In: Proceedings of 58th ECTC 2008, Orlando, p. 330 (2008)
- Y.-S. Lai, J.-M. Song, Electromigration reliability with respect to Cu content in solder joint system. In: Proceedings of 58th ECTC 2008, Orlando, p. 1160 (2008)
- J.W. Jang, L.N. Ramanathan, D.R. Frear, Electromigration behavior of lead-free solder flip chip bumps on NiP/Cu metallization. *J. Appl. Phys.* **103**(12), 123506 (2008)
- S. Peng, L. Li, A comparison study of electromigration performance of Pb-free flip chip solder bumps. In: Proceedings of 59th ECTC 2009, San Diego, p. 1456 (2009)
- L.D. Chen, M.L. Huang, S.M. Zhou, Effect of electromigration on intermetallic compound formation in line-type Cu/Sn/Cu and Cu/Sn/Ni interconnects. In: Proceedings of 60th ECTC 2010, Las Vegas, p. 176 (2010)
- J.K. Dong, Wook Kim, J. Lee, M.-J. Lee, et al., Evaluation of electromigration (EM) life of ENEPIG and CuSOP surface finishes with various solder bump materials. In: Proceedings of 60th ECTC 2010, Las Vegas, p. 1841 (2010)
- K.H. Kuo, J. Lee, C. Stan, et al., Electromigration performance of printed Sn0.7Cu bumps with immersion tin surface finishing for flip chip applications. In: Proceedings of 62th ECTC 2012, Sparks, p. 698 (2012)
- K. Lee, K.S. Kim, Y. Tsukada et al., Effects of the crystallographic orientation of Sn on the electromigration of Cu/Sn-Ag-Cu/Cu ball joints. *J. Mater. Res.* **26**(3), 467 (2011)
- Y. Yamanaka, H. Nishikawa, H. Taguchi et al., Effect of magnetic flux density on Sn crystallographic orientation in a solder joint system. *J. Mater. Sci.* **27**, 3710 (2016)
- T. Kadoguchi, K. Gotou, K. Yamanaka, et al., Electromigration behavior in Cu/Ni-P/Sn–Cu based joint system with low current density. *Microelectron. Reliab.* **55**, 2554 (2015)

30. M.A. Matin, E.W.C. Coenen, W.P. Vellinga, M.G.D. Geers, Correlation between thermal fatigue and thermal anisotropy in a Pb-free solder alloy. *Scr. Mater.* **53**, 927 (2005)
31. T.R. Bieler, Influence of Sn grain size and orientation on the thermomechanical response and reliability of Pb-free solder joints. *IEEE Trans. CPT* **31**(3), 370 (2008)
32. B.F. Dyson, T.R. Anthony, D. Turnbull, Interstitial diffusion of copper in tin. *J. Appl. Phys.* **38**(8), 3408 (1967)
33. D.C. Yeh, H.B. Huntington, Extreme fast-diffusion system: nickel in single-crystal tin. *Phys. Rev. Lett.* **53**, 1469 (1984)